ASPS Conference Proceedings 1: 1057-1063 (2022)

Proceedings of

12th Structural Engineering Convention-An International Event (SEC 2022)

Available at https://asps-journals.com/index.php/acp

Empirical Validation of Free Vibration of Sagging Cables

Pankaj Kumar [1, *], Abhijit Ganguli [2], Gurmail S. Benipal [3]

[1] Department of Civil Engineering, Assistant Professor, Madhav Institute of Technology and Science, Gwalior 474005, India
[2] Department of Civil Engineering, Associate Professor, Indian Institute of Technology Tirupati 517506, India
[3] Department of Civil Engineering, Professor, Indian Institute of Technology Delhi 110016, India

Paper ID - 070124

Abstract

Sagging cables lack unique natural state, but possess unique equilibrium state under sustained loads. However, for the purpose of predicting their dynamic response, the static equilibrium state of heavy cables under self-weight is assumed to be their initial state. The theory of sagging elastic cables presented earlier by the Authors pertains to weightless cables carrying nodal masses apart from static and inertial forces. For applying the proposed theory for sagging heavy cables, the cable is divided into ten segments of equal length. The initial equilibrium configuration of the cable fixed at both the ends is determined by the weights of these lumped nodal masses applied at ten nodes with one end fixed. The stiffness matrix of the cable is determined from tangent configurational flexibility matrix and tangent elastic flexibility matrix of twenty degree of freedom system. The cable tied at both the ends in an equilibrium state is set into motion by releasing it at one end. The theoretically predicted response of the cable is compared with the experimental data from the two investigations. The first experimental investigation by Fried pertains to the planar undamped vibrations of a sagging elastic cable, in which cable is released from its right end and its configurations are plotted at regular time intervals of 0.001s. In the second investigation by Koh, Zhang and Quek, the configurations of a different cable at regular time intervals of 0.125s during half the vibration cycle is measured. The dynamic tensile force at the fixed end has also been predicted in the latter case. The theoretical prediction of the evolving cable configuration have been found to be compatible with experimental data.

Keywords: Heavy cable, sagging elastic cable, flexibility matrix, experimental investigations, dynamic tensile force

1. Introduction

Cables are popular structural materials used in diverse areas like transportation, power transmission, cranes, trolleys, marine environment, entertainment, etc. Most of the theoretical investigations deal with single heavy sagging cables with or without concentrated loads. The deformed equilibrium state under self-weight and applied constant point loads is assumed to play the role of reference state. Response to additional applied forces is presented in terms of displacements from this reference state. The undeformed and deformed configurations of the elastic cables are defined by following the Lagrangian approach. The position of a material point on the cable is identified by its distance measured along its undeformed cable length from the chosen end. In the discrete formulation, their incremental constitutive equations are stated using their tangent stiffness matrices. Generally, the tangent stiffness matrix is obtained as the sum of tangent elastic and geometric stiffness matrices [1,2]. The tension-extension relations for the elastic cables are generally assumed to be linear. The tensile force at any point on the cable is determined by the local strain itself defined by change in length per unit undeformed length [3,4,5,6].

A theory of single sagging elasto-flexible cables is proposed by the Authors in which the instantaneous magnitudes of the cable tensile forces introduced by the instantaneous applied forces are determined by conducting static analysis in the instantaneous deformed state configuration. Incremental second order differential equations of motion of these MDOF structures are stated in terms of the tangent stiffness matrices, nodal placement, nodal velocity and nodal acceleration increments [7].

In the discrete formulation, the nodal coordinates or placements are generally defined in reference to the chosen Cartesian coordinate system. In view of this, this theory is called Placement Model. In contrast, the Authors' derived the constitutive relations assuming nodal forces as the primary variables [7] referred as Force Model. Further, the Placement Model differs from the conventional displacement method used for the matrix analysis of structures. Of course, in both the Placement and the Force Models, the nodal deformed placements constitute the primary kinematic variables in the equation of motion. The proposed Force Model by the Author's is compared with the existing Placement Model [8].

It must be remembered that the Placement Model has been developed for the cables sustaining self-weight, while Force Model is proposed for the weightless cables. It is

*Corresponding author. Tel: +919968270408; E-mail address: pankaj437@gmail.com

Published online: December 19, 2022
doi:10.38208/acp.v1.620

decided to compare the predictions of the structural response of the weightless sagging planar cables. In view of this, first of all, the Placement Model is recast for these weightless sagging cables subjected to point loads.

To recapitulate, the theory of planar sagging elastic cables proposed here assumes the cables to be weightless as well as massless. In contrast, the real cables do possess distributed mass and so weight in the gravitational field of the earth. Further, in contrast to conventional elastic structures, perfectly flexible cables lack unique passive natural reference state configuration, though their equilibrium state configuration is unique. Thus, in the absence of additional applied loads, the sagging cables exhibit catenary configuration under the self-weight caused by ever-present and ubiquitous gravitational field. In view of this, it is extremely difficult, if not altogether impossible, to conduct experiments to validate the theory of weightless cables.

Many researchers have undertaken experimental investigations on cables and cable structures. These experimental investigations deal with wind and rain effects, cables in marine environment, support excitation, longitudinal excitations, vibration control, taut cables, parametric resonance, effect of flexural rigidity, spatial motion, cable trusses, etc. Experimental data from two investigations is available which can serve the desired purpose [9,10]. Both of these investigations deal with heavy sagging elastic chains or cables fixed at both the ends at the same level. In the absence of any additional applied forces, the cable assumes a catenary shape due to uniformly distributed self-weight. The cable in such an equilibrium is set into motion by releasing it from one of the ends. These experiments are characterized by very large amplitude motion of the cable with very little tensile force near its free end. In the first experiment, the free-fall motion of the chain is recorded on a video camera [9]. In the second study, tensile force at the fixed end of the vibrating neoprene rubber cable has been determined using strain gauges located near that end [10].

In the proposed theory of cables [7] analytical expressions are derived only for 2-node 4-DOF cable structures. To model the distributed mass, weight and forces in the experimental cables, new expressions for the 10-node 20-DOF planar elastic sagging cable are developed. A comparison of the theoretical predictions of motion of cables with experimental data is presented here.

2. Computational Model

The theory of sagging elastic cables proposed [7] is modified here for the purpose of predicting the observed dynamic response. The theory of sagging elastic cables presented earlier pertains to weightless cables carrying nodal masses apart from static and inertial forces. More significantly, explicit analytical derivation pertains to cables tied at both the ends and supporting point masses and forces at two nodes. In contrast, the cables used in these experiments are tied only at one end and also have uniformly distributed mass, self-weight and inertial forces. For applying the proposed theory, the sagging cable is divided into ten segments of equal length as shown in Fig. 1.

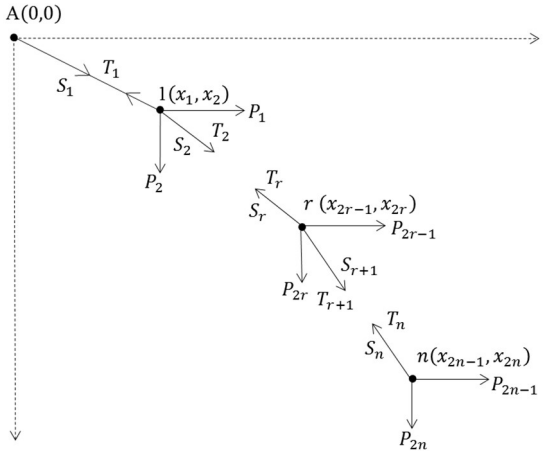

Fig. 1 Cable tied at one end ($n = 10$)

The initial equilibrium configuration of the cable fixed at both the ends is determined by the weights of these nodal masses. Also, the nodal weights are the applied constant nodal force acting on the vibrating cable. Otherwise for all computation purposes, the cable itself is assumed to be massless and weightless. The expression for tensile forces (T_r) and the nodal coordinates ($x_{2r-1},\ x_{2r}$)are derived here for the cable with n segment ($n = 10$) having segment length (s_r).

$$T_r = \sqrt{\begin{matrix}(P_{2r-1} + P_{2r+1} + P_{2r+3} \dots + P_{2n-1})^2 \\ +(P_{2r} + P_{2r+2} + P_{2r+4} + \cdots + P_n)^2\end{matrix}} \tag{1}$$

$$\begin{aligned} x_{2r-1} &= x_{2r-3} + \frac{S_r}{T_r}(P_{2r-1} + P_{2r+1} + P_{2r+3} \dots \\ &\quad + P_{2n-1}) \\ x_{2r} &= x_{2r-2} + \frac{S_r}{T_r}(P_{2r} + P_{2r+2} + P_{2r+4} + \cdots + P_n) \end{aligned} \tag{2}$$

For $r = 1$, the coordinate (x_{-1}, x_0) represents the coordinate of the fixed node $(0, 0)$. The tangent configurational flexibility matrix coefficients ($D_{ij} = \partial x_i/\partial P_j$) are derived. Total elastic complementary energy of the structure is expressed in terms of nodal forces as $\Omega_e = \sum_{i=1}^{10} \frac{T_i{}^2\, S_i}{2AE}$. The small elastic displacements ($u_i = \partial\Omega_e/\partial P_i$) and the tangent elastic flexibility matrix coefficients ($f_{ij} = \partial u_i/\partial P_j$) are obtained. The expression for f_{ij} matrix of equal segment lengths (S) are determined.

The cable is in equilibrium with the nodal loads applied at 10 nodes with one end fixed at A. The cable configuration with their nodal coordinates are determined using equilibrium equations at each node. The applied constant nodal force vector (F_0) causing vibration is given by vertical gravitational force acting at the nodes as

$$\begin{aligned} F_0 = [0;\ mg;\ 0;\ mg;\ 0;\ mg;\ 0;\ mg;\ 0;\ mg; \\ 0;\ mg;\ 0;\ mg;\ 0;\ mg;\ 0;\ mg/2 \end{aligned} \tag{3}$$

The mass matrix M is presented as 20 × 20 matrix as (4)

$$M = \begin{bmatrix} m & 0 & 0 & 0 & 0 & 0 & 0 & 0 & 0 & 0 & 0 & 0 & 0 & 0 & 0 & 0 & 0 & 0 & 0 & 0 \\ 0 & m & 0 & 0 & 0 & 0 & 0 & 0 & 0 & 0 & 0 & 0 & 0 & 0 & 0 & 0 & 0 & 0 & 0 & 0 \\ 0 & 0 & m & 0 & 0 & 0 & 0 & 0 & 0 & 0 & 0 & 0 & 0 & 0 & 0 & 0 & 0 & 0 & 0 & 0 \\ 0 & 0 & 0 & m & 0 & 0 & 0 & 0 & 0 & 0 & 0 & 0 & 0 & 0 & 0 & 0 & 0 & 0 & 0 & 0 \\ 0 & 0 & 0 & 0 & m & 0 & 0 & 0 & 0 & 0 & 0 & 0 & 0 & 0 & 0 & 0 & 0 & 0 & 0 & 0 \\ 0 & 0 & 0 & 0 & 0 & m & 0 & 0 & 0 & 0 & 0 & 0 & 0 & 0 & 0 & 0 & 0 & 0 & 0 & 0 \\ 0 & 0 & 0 & 0 & 0 & 0 & m & 0 & 0 & 0 & 0 & 0 & 0 & 0 & 0 & 0 & 0 & 0 & 0 & 0 \\ 0 & 0 & 0 & 0 & 0 & 0 & 0 & m & 0 & 0 & 0 & 0 & 0 & 0 & 0 & 0 & 0 & 0 & 0 & 0 \\ 0 & 0 & 0 & 0 & 0 & 0 & 0 & 0 & m & 0 & 0 & 0 & 0 & 0 & 0 & 0 & 0 & 0 & 0 & 0 \\ 0 & 0 & 0 & 0 & 0 & 0 & 0 & 0 & 0 & m & 0 & 0 & 0 & 0 & 0 & 0 & 0 & 0 & 0 & 0 \\ 0 & 0 & 0 & 0 & 0 & 0 & 0 & 0 & 0 & 0 & m & 0 & 0 & 0 & 0 & 0 & 0 & 0 & 0 & 0 \\ 0 & 0 & 0 & 0 & 0 & 0 & 0 & 0 & 0 & 0 & 0 & m & 0 & 0 & 0 & 0 & 0 & 0 & 0 & 0 \\ 0 & 0 & 0 & 0 & 0 & 0 & 0 & 0 & 0 & 0 & 0 & 0 & m & 0 & 0 & 0 & 0 & 0 & 0 & 0 \\ 0 & 0 & 0 & 0 & 0 & 0 & 0 & 0 & 0 & 0 & 0 & 0 & 0 & m & 0 & 0 & 0 & 0 & 0 & 0 \\ 0 & 0 & 0 & 0 & 0 & 0 & 0 & 0 & 0 & 0 & 0 & 0 & 0 & 0 & m & 0 & 0 & 0 & 0 & 0 \\ 0 & 0 & 0 & 0 & 0 & 0 & 0 & 0 & 0 & 0 & 0 & 0 & 0 & 0 & 0 & m & 0 & 0 & 0 & 0 \\ 0 & 0 & 0 & 0 & 0 & 0 & 0 & 0 & 0 & 0 & 0 & 0 & 0 & 0 & 0 & 0 & m & 0 & 0 & 0 \\ 0 & 0 & 0 & 0 & 0 & 0 & 0 & 0 & 0 & 0 & 0 & 0 & 0 & 0 & 0 & 0 & 0 & m/2 & 0 & 0 \\ 0 & 0 & 0 & 0 & 0 & 0 & 0 & 0 & 0 & 0 & 0 & 0 & 0 & 0 & 0 & 0 & 0 & 0 & m/2 & 0 \end{bmatrix}$$

The stiffness matrix of the cable is determined from the tangent configurational flexibility matrix and tangent elastic flexibility matrix as $K = \left(D_{ij} + f_{ij}\right)^{-1}$. The cable shape (displacement response) is obtained by numerical integration of third order differential equation of motion using modified Runge-Kutta Method.

In the experimental investigations, a cable tied at both the ends in an equilibrium state is set into motion by releasing it at one end. As the cable in its initial equilibrium state lies in a vertical plane, it is expected to vibrate in the same plane. However, it should be noted that the resistance offered by these cables under self-weight against motion in the direction normal to the plane of vibration is quite low. It may so happen that, while releasing the cable at one end, the cable may be subjected to an unintended force in that transverse direction. In such a case, the motion of the cable will be spatial, not planar as assumed here during experimentation as well as theoretical predictions.

2.1 Empirical Validation I: Fried (1982)

The first experimental investigation pertains to the planar undamped vibrations of a sagging elastic cable with the following numerical details:
Cable length, S = 1.00 m;
Horizontal span, L = 0.881 m;
Sag/ span ratio = 0.207;
Axial stiffness of the cable section, $EA = 1.57 \times 10^5$ N

Relevant structural properties of cable are not provided in Fried's Paper [9]. However, based upon their static analysis Koh, Zhang and Quek [10] have estimated the required properties as follows which are compatible with the above sag/span ratio. The cable properties required for its static and dynamic analysis are determined in the dimensionless form as

$$\bar{x} = \frac{x}{S}; \quad \bar{y} = \frac{y}{S}; \quad \bar{f}_x = \frac{f_x}{EA}; \quad \bar{t} = \frac{t}{\sqrt{S/g}}; \quad \mu = \frac{\rho g S}{E} \qquad (5)$$

Using the given value (μ = 1.55× 10^{-2}), the mass per unit length of the cable is obtained as $\rho A = \sqrt{\mu EA/gs} = 281.57\ kg/m$. The nodal mass ($m$) is taken as $\rho AS/n$. The initial cable configuration is determined by static analysis of the cable subjected to applied nodal force vector ($\bar{F}$) as

$$\bar{F} = [0;\ mg;\ 0;\ mg; 0;\ mg; 0;\ mg;\ 0;\ mg;\ 0;\ mg; \\ 0;\ mg;\ 0;\ mg;\ 0;\ mg; 1373.2\ ; -4.5mg] \qquad (6)$$

The nodal coordinates of eleven nodes are obtained as (0, 0); (0.0741, 0.0671); (0.1559, 0.1247); (0.2452, 0.1696); (0.3410, 0.1985); (0.4405, **0.2085**); (0.5400, 0.1985); (0.6357, 0.1696), (0.7251, 0.1247); (0.8068, 0.0671); (0.8810, 0.0000) m. From the obtained nodal coordinates, the maximum sag of the cable is obtained as **0.2085** m.

Here, forces $\bar{F}_{19}$ and $\bar{F}_{20}$ acting at the free end ($n = 10$) are determined as follows: The vertically upward force $\bar{F}_{20}$ balances half of the self-weight of the cable except the weight assigned to the node 10, i.e., $\bar{F}_{20} = (-10\ mg/2 + mg/2) = -4.5\ mg$. The horizontal force component $\bar{F}_{19}$ is estimated from the computation that the initial coordinates of the tenth node equals $(L, 0)$. The coordinate system has is origin at the fixed end of the cable.

After the cable is released from its right end, its configurations are plotted at regular time intervals of 0.001s [9]. This experimental data on configurations of the vibrating cable is presented in Fig. 2 in the form of dimensi-

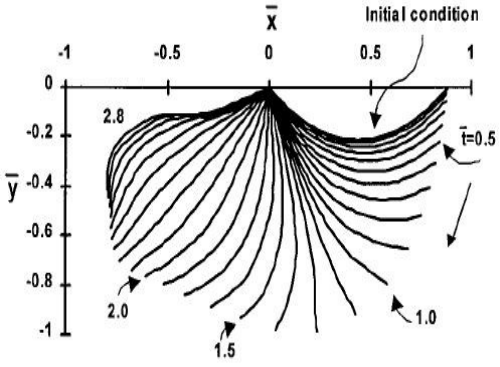

(a) $\bar{t}$ = 0 to 2.8

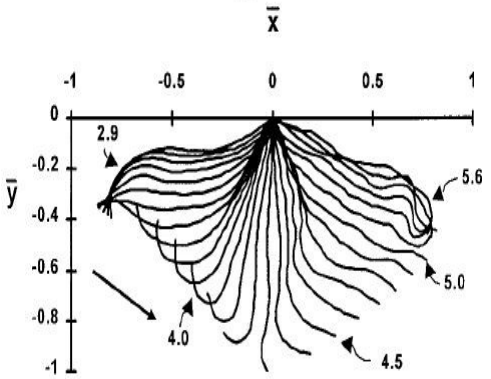

(b) $\bar{t}$ = 2.9 to 5.6

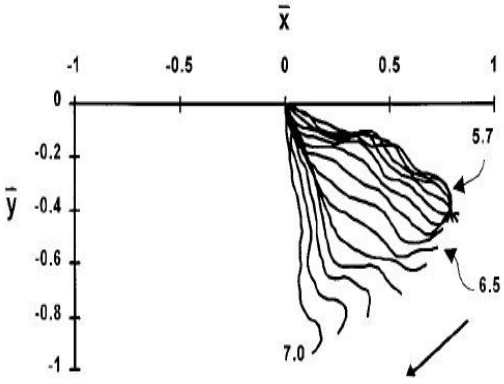

(c) $\bar{t}$ = 5.7 to 7.0

Fig. 2 Observed cable configurations by Fried (1982)

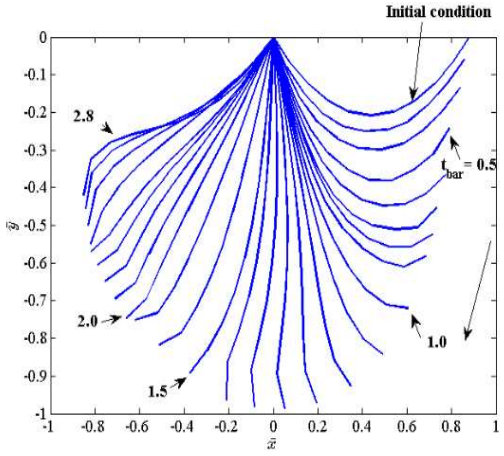

(a) $\bar{t}$ = 0 to 2.8

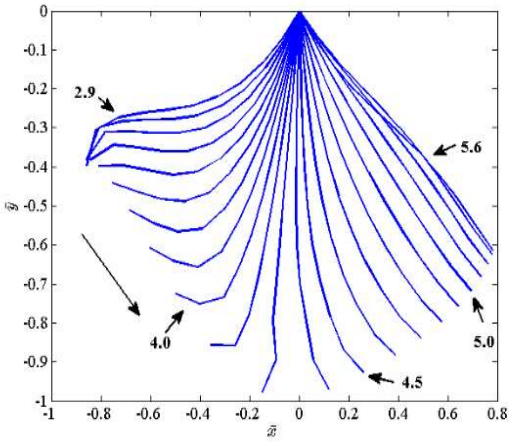

(b) $\bar{t}$ = 2.9 to 5.6

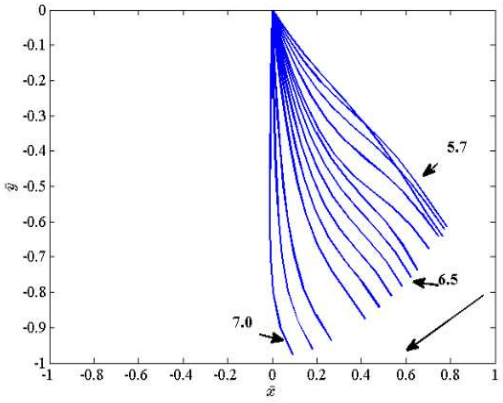

(c) $\bar{t}$ = 5.7 to 7.0

Fig. 3 Predicted cable configurations

-onless variables ($\bar{x}$, $\bar{y}$, $\bar{t}$) by Koh, Zhang and Quek at regular normalized time intervals ($\bar{t}$) of 0.1. In Fig. 3, the vibrating cable configurations are shown at unit normalized time intervals [10]. It can be observed that the normalized time period of the structure is about 6 which equals about 1.8 s. In this paper, the theoretical predictions are compared with these data.

To recapitulate, the period of free vibration of a rigid pendulum of length S and with lumped mass at its free end given by the formula $2\pi\sqrt{S/g}$ turns out to be 2.006 s for the pendulum of unit length. It is interesting to note that that the period of the pendulum of the same length but with distributed mass is slightly lesser. For ease of comparison, the configurations of the moving cable observed at regular intervals by Fried [9] and reproduced by Koh, Zhang and Quek [10] are presented in Fig. 2. The predicted cable configurations for the first seven normalised time units shown in Fig. 3 can be observed to be quite accurate. The normalised period of damped vibration is obtained as 5.6 s. The characteristic curling of the free end of the falling cable is also predicted accurately.

The cable tension at fixed end was not recorded by Fried [9]. The normalised cable tension as predicted later by Koh, Zhang and Quek [10] for the Fried cable is reproduced in Fig. 4 (a). The variation of normalised tensile force in segment near the fixed end of the cable as predicted using the theory proposed herein is depicted in Fig. 4 (b). The present theoretical prediction can be observed to be closure to Box Scheme predictions.

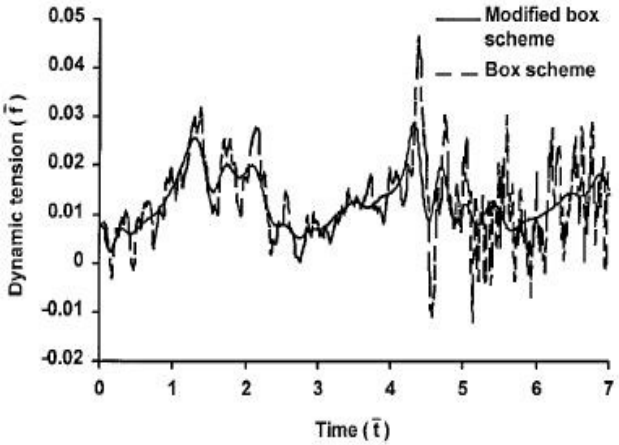

(a) Cable tension by Koh, Zhang and Quek (1999)

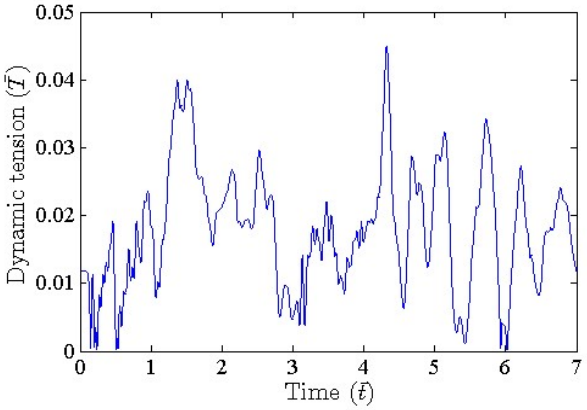

(b) Predicted cable tension

Fig. 4 Cable tension at fixed end

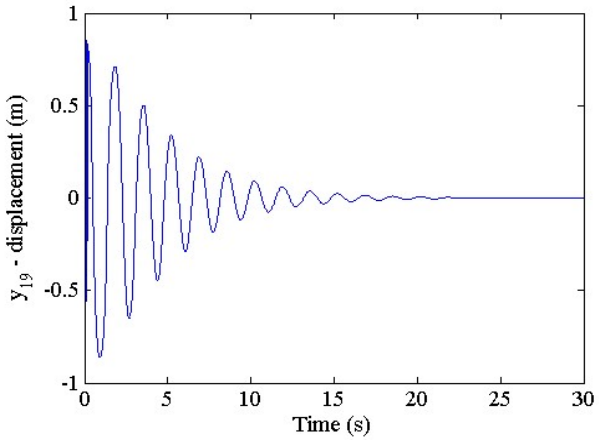

(a) y_{19} – coordinate

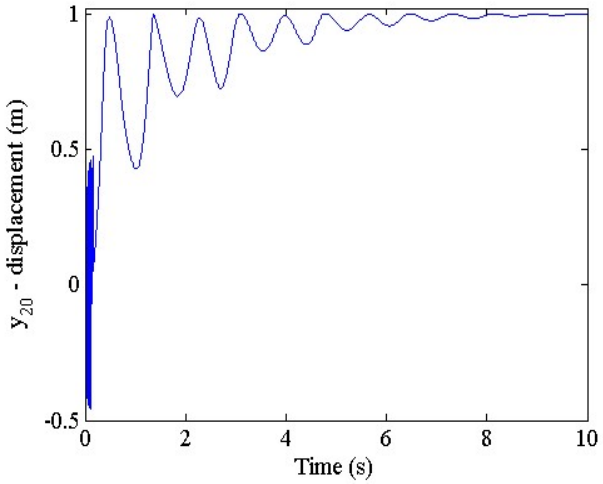

(b) y_{20} - coordinate

Fig. 5 Response of free end

Fig. 5 shows the predicted variation of the nodal coordinates of the free end of the vibrating cable. Starting from the initial cable configuration with free end coordinates $(L, 0)$, the damped vibrating cable asymptotically attains, as expected, a vertical configuration with free end coordinates (0, y_{20}), where $y_{20} = x_{20} + u_{20}$ with y_{20} = 1.0088 m, x_{20} =1.00 m and u_{20} = 0.0088 m.

2.2 Empirical Validation II: Koh, Zhang and Quek (1999)

The second experimental investigation pertains to the planar vibrations of a sagging elastic cable with the following numerical details:
Cable length, S = 2.022 m;
Horizontal span, L = 1.805 m;
Diameter of cable section = 25 mm;
Area of cross section, A = 4.9087× 10^{-4} m^2;
Young's modulus of elasticity, E = 3.14× 10^6 N/m^2;
Axial stiffness of the cable section, = 1541.33 N;
Material density, $\rho = 1430\ kg/m^3$;
Mass per unit length, ρA = 0.7019 kg/m;
Nodal force vectors F_0 and $\bar{F}$ are presented below:

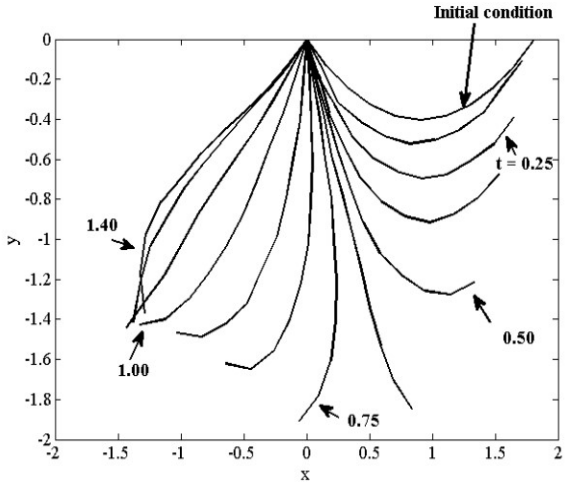

Fig. 6 Predicted cable configurations

$$F_0 = [0;\ mg;\ 0;\ mg;\ 0;\ mg;\ 0;\ mg;\ 0;\ mg;\ 0;\ mg;\ 0;\ mg;\ 0;\ mg;\ 0;\ mg/2];$$
$$\bar{F} = [0;\ mg;\ 0;\ mg;\ 0;\ mg;\ 0;\ mg;\ 0;\ mg;\ 0;\ mg;\ 0;\ mg;\ 0;\ mg;\ 7.42\ ;-4.5mg]; \quad (7)$$

The cable configuration at initial state are calculated with their nodal coordinates of eleven nodes as (0, 0); (0.1545, 0.1304); (0.3235, 0.2414); (0.5066, 0.3273); (0.7012, 0.3821); (0.9025, **0.4010**); (1.1038, 0.3821); (1.2985, 0.3273); (1.4815, 0.2414); (1.6505, 0.1304); (1.8050, 0.0000) m. Predicted sag/span ratio is obtained here as 0.4010 m.

The configurations of the cable at regular time intervals (0.125 s) during half the vibration cycle as predicted by the proposed theory are presented in Fig. 6. The experimental data for the Koh, Zhang and Quek cable required for comparison is not available. The predicted variation of cable configurations with progress of time is similar to the observed qualitative evolution of Fried-cable configurations shown above in Fig. 2 (a).

It should be noted that the normalised tensile force at any point equals the axial elastic strain at that point. Fig. 7 (a) shows the temporal variation of elastic strain at fixed end observed at two different data acquisition rates. As shown in Fig. 8 (a), the variation of elastic strain in the first segment predicted here for the corresponding time intervals is similar. The observed variation of tensile forces at the fixed end of the cable is depicted in Fig. 7 (b) and Fig. 7 (c) at different data acquisition rates. The theoretically predicted tensile forces at fixed end shown in Fig. 8 (b) and Fig. 8 (c) display similar qualitative trend. From Fig. 8 (b), dynamic tension is seen to tend to approximately equal the weight (13.22 N) of masses at all the nodes except the fixed end.

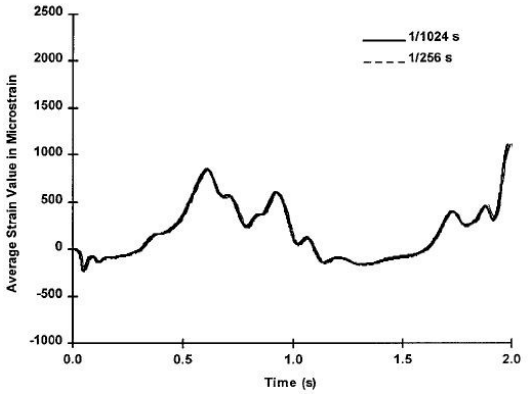

(a) Average strain value

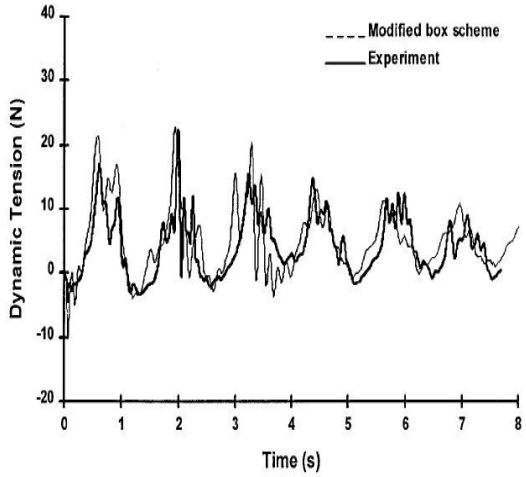

(b) Dynamic tension ($\Delta t = 1/256\ s$)

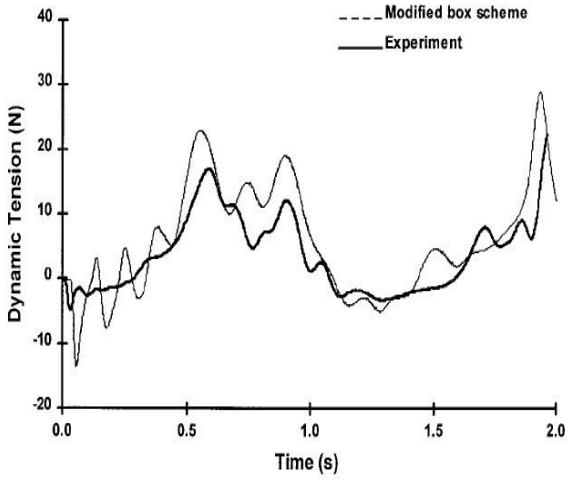

(c) Dynamic tension ($\Delta t = 1/1024\ s$)

Fig. 7 Response at fixed end (Koh, Zhang and Quek, 1999)

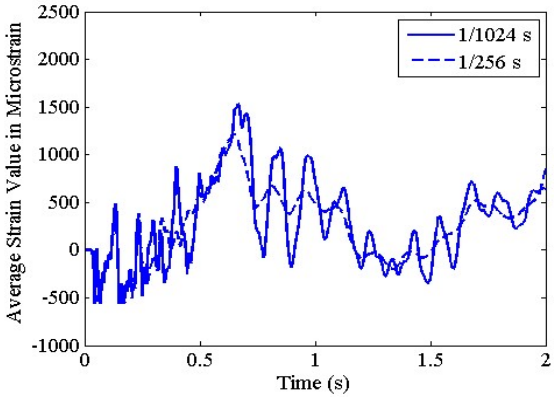

(a) Average strain value

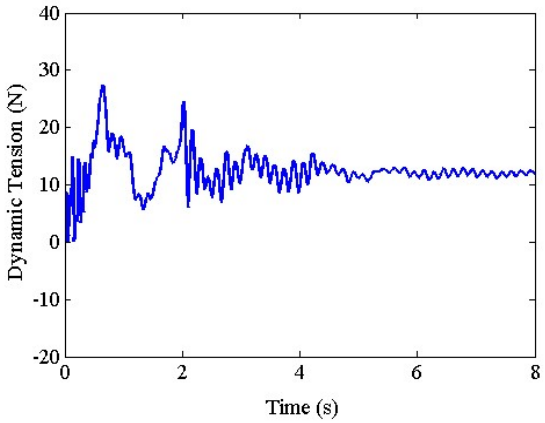

(b) Dynamic tension ($\Delta t = 1/256\ s$)

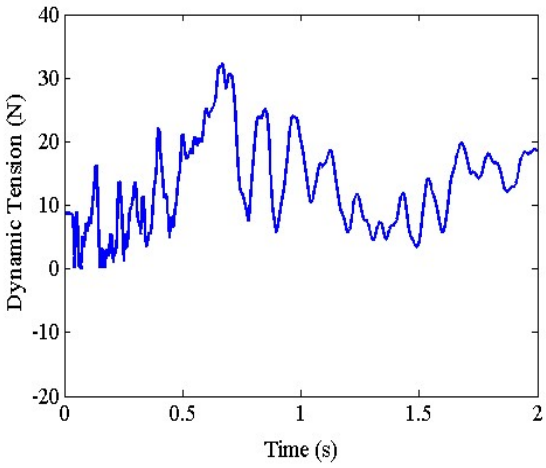

(c) Dynamic tension ($\Delta t = 1/1024\ s$)

Fig. 8 Predicted response at fixed end

3. Conclusions

One of the qualitative aspects of observed response of test cables experiencing free-fall is identified as characteristic curling of the cables near their free end. It should be noted that, in real test cables, the tensile force and hence stiffness of cables in that region is very low. Many researchers have assigned, in the computational algorithms, some flexural rigidity to the cable to eliminate the possible numerical

instabilities caused by low tension. Here, such curling up of cables near free end is predicted assuming the cable to be perfectly flexible.

To recapitulate, the test cables have distributed mass and are subjected to distributed forces. In contrast, the theoretical predictions are based upon discrete formulation assuming weightless cable with nodal masses and forces. The cable is divided into ten segments of equal length. It is well-known that the accuracy of discrete formulations can be increased further by increasing the number of segments. However, the analytical derivations required for predicting the response are expected to become more complex with increase in number of segments and nodes. It should be noted that the tensile force for the Koh, Zhang and Quek cable predicted here actually pertains to the cable segment nearest to the fixed but end but not at the fixed end. Shorter cable segments chosen for theoretical prediction is expected to increase its accuracy.

It is well-known that the distributed self-weight and inertial forces distributed on the curved cable segments or finite elements of an actual cable affect their stiffness. Many attempts have been made to incorporate the consequent nonlinearity of element force-displacement relations. It is worth mentioning that, in the proposed theory, the cable segments are assumed to be straight ignoring the effect of distributed forces on a segment on its stiffness. It is indeed creditable that, despite such a simplification, the theoretical predictions are still satisfactory.

Disclosures

Free Access to this article is sponsored by SARL ALPHA CRISTO INDUSTRIAL.

References

1. Thai, H.T. and Kim, S.E. (2008). “Second-order inelastic dynamic analysis of three-dimensional cable-stayed bridges.” Steel Structures, 8: 205-214.
2. Santos, H.A.F.A. and Paulo, C.I.A. (2011). “On a pure complementary energy principle and a force-based finite element formulation for non-linear elastic cable.” International Journal of Non-linear Mechanics, 46: 395-406.
3. Luongo, A., Rega, G. and Vestroni, F. (1984). “Planer non-linear free vibrations of an elastic cable.” Int. J. Non-Linear Mech., 19: 39-52.
4. Antman, S.S. (2005). Nonlinear problems of elasticity. Springer.
5. Lacarbonara, W. (2013). Nonlinear structural mechanics: Theory dynamical phenomenon and modelling, Springer.
6. Greco, L., Impollonia, N. and Cuomo, M. (2014). “A procedure for the static analysis of cable structures following elastic catenary theory.” HAL archieves-ouvertes.
7. Kumar P., Ganguli A. and Benipal G.S. (2016). “Theory of weightless sagging elasto-flexible cables.” Latin American Journal of Solids and Structures, (13): 155-174.
8. Kumar P., Ganguli A. and Benipal G.S. (2019). “Comparative assessment of the contending force and placement methods for weightless sagging cables.” Asian Journal of Civil Engineering DOI: https://doi.org/10.1007/s42107-019-00163-9.
9. Fried, I. (1982). “Large deformation static and dynamic finite element analysis of extensible cables,” Computers and Structures, 15(3): 315-319.
10. Koh, C.G, Zhang, Y. and Quek, S.T. (1999). “Low-tensioned cable dynamics: numerical and experimental Studies.” J. of Eng. Mechanics, 125(3): 347-354.